

# REPORT DOCUMENTATION PAGE

Form Approved  
OMB NO. 0704-0188

Public Reporting burden for this collection of information is estimated to average 1 hour per response, including the time for reviewing instructions, searching existing data sources, gathering and maintaining the data needed, and completing and reviewing the collection of information. Send comment regarding this burden estimates or any other aspect of this collection of information, including suggestions for reducing this burden, to Washington Headquarters Services, Directorate for information Operations and Reports, 1215 Jefferson Davis Highway, Suite 1204, Arlington, VA 22202-4302, and to the Office of Management and Budget, Paperwork Reduction Project (0704-0188,) Washington, DC 20503.

1. AGENCY USE ONLY ( Leave Blank)		2. REPORT DATE January 6, 2006	3. REPORT TYPE AND DATES COVERED July 1, 2002 - December 31, 2005	
4. TITLE AND SUBTITLE The Analysis of Thermal Stability and Crystallization of Structural Amorphous Alloys			5. FUNDING NUMBERS DAAD 19-02-1-0245	
6. AUTHOR(S) J. H. Perepezko				
7. PERFORMING ORGANIZATION NAME(S) AND ADDRESS(ES) University of Wisconsin - Madison 1500 Engineering Drive, Madison, WI 53711			8. PERFORMING ORGANIZATION REPORT NUMBER	
9. SPONSORING / MONITORING AGENCY NAME(S) AND ADDRESS(ES) U. S. Army Research Office P.O. Box 12211 Research Triangle Park, NC 27709-2211			10. SPONSORING / MONITORING AGENCY REPORT NUMBER 43777.1-MS	
11. SUPPLEMENTARY NOTES The views, opinions and/or findings contained in this report are those of the author(s) and should not be construed as an official Department of the Army position, policy or decision, unless so designated by other documentation.				
12 a. DISTRIBUTION / AVAILABILITY STATEMENT Approved for public release; distribution unlimited.			12 b. DISTRIBUTION CODE	
13. ABSTRACT (Maximum 200 words) Please see continuation sheet for full text of abstract.				
14. SUBJECT TERMS metallic glass, nanocrystallization, amorphous alloy, kinetics			15. NUMBER OF PAGES 26	
			16. PRICE CODE	
17. SECURITY CLASSIFICATION OR REPORT <b>UNCLASSIFIED</b>	18. SECURITY CLASSIFICATION ON THIS PAGE <b>UNCLASSIFIED</b>	19. SECURITY CLASSIFICATION OF ABSTRACT <b>UNCLASSIFIED</b>	20. LIMITATION OF ABSTRACT <b>UL</b>	

NSN 7540-01-280-5500

Standard Form 298 (Rev.2-89)  
Prescribed by ANSI Std. 239-18  
298-102

Enclosure 1

---

**REPORT DOCUMENTATION PAGE (SF298)**  
**(Continuation Sheet)**

---

Controlled synthesis of bulk nanostructured volumes comprised of a high density ( $10^{21} - 10^{23} \text{ m}^{-3}$ ) of nanocrystals ( $7 - 20 \text{ nm}$ ) dispersed throughout an amorphous matrix requires a thorough understanding of the primary crystallization reactions responsible for their transformation. The primary crystallization of Al from amorphous Al alloys generally is observed in the competitive kinetics of devitrification in spite of a reduced driving free energy, which results from a hypereutectic composition within the amorphous matrix. Differential scanning calorimetry (DSC) studies of Al<sub>92</sub>Sm<sub>8</sub> and Al<sub>87</sub>Ni<sub>10</sub>Ce<sub>3</sub> alloys, based upon sub-T<sub>g</sub> annealing treatments, demonstrate a strong sensitivity of the primary crystallization onset and reaction enthalpy to thermal history and the as-quenched state. Calorimetry investigations, careful analysis of nanocrystal size distributions, small angle x-ray scattering studies, and fluctuation electron microscopy investigations of Al<sub>92</sub>Sm<sub>8</sub> MSR (melt spun ribbon) following sub-T<sub>g</sub> anneals reveal a transient, decaying nucleation rate and a limited supply of heterogeneous nucleation sites that may originate from the medium range order (MRO) detected in the as-quenched state.

In Al<sub>88</sub>Ni<sub>8</sub>Sm<sub>4</sub> melt-spun ribbon (MSR), incremental substitutions of Cu for Ni (0 – 1 at%) affect the thermal stability of the material (crystallization onset shifts to lower temperature) and refine the size of the primary phase nanocrystals. However, continuous heating calorimetry measurements indicate that the primary crystallization enthalpy remains approximately constant with increased Cu substitution. From a structural analysis standpoint, quantitative microstructure examinations applied in parallel with calorimetry measurements have been employed to characterize the as-quenched volume of MSR samples. The kinetics behavior highlights the important role of the as-synthesized amorphous structure, modification of local structural arrangements, reaction pathways and transient conditions on the evolution of nanoscale microstructures during primary crystallization.

## *Table of Contents*

Abstract	1 – 2
Scientific Progress and Accomplishments	3 – 17
References	18 – 19
Figures	20 – 22
Publications of the Current Program	23 – 25
Scientific Personnel	26

## ***Abstract***

Controlled synthesis of bulk nanostructured volumes comprised of a high density ( $10^{21} - 10^{23} \text{ m}^{-3}$ ) of nanocrystals (7 – 20nm) dispersed throughout an amorphous matrix requires a thorough understanding of the primary crystallization reactions responsible for their transformation. The primary crystallization of Al from amorphous Al alloys generally is observed in the competitive kinetics of devitrification in spite of a reduced driving free energy, which results from a hypereutectic composition within the amorphous matrix. Differential scanning calorimetry (DSC) studies of  $\text{Al}_{92}\text{Sm}_8$  and  $\text{Al}_{87}\text{Ni}_{10}\text{Ce}_3$  alloys, based upon sub- $T_g$  annealing treatments, demonstrate a strong sensitivity of the primary crystallization onset and reaction enthalpy to thermal history and the as-quenched state. Calorimetry investigations, careful analysis of nanocrystal size distributions, small angle x-ray scattering studies, and fluctuation electron microscopy investigations of  $\text{Al}_{92}\text{Sm}_8$  MSR (melt spun ribbon) following sub- $T_g$  anneals reveal a transient, decaying nucleation rate and a limited supply of heterogeneous nucleation sites that may originate from the medium range order (MRO) detected in the as-quenched state.

In  $\text{Al}_{88}\text{Ni}_8\text{Sm}_4$  melt-spun ribbon (MSR), incremental substitutions of Cu for Ni (0 – 1at%) affect the thermal stability of the material (crystallization onset shifts to lower temperature) and refine the size of the primary phase nanocrystals. However, continuous heating calorimetry measurements indicate that the primary crystallization enthalpy remains approximately constant with increased Cu substitution. From a structural analysis standpoint, quantitative microstructure examinations applied in parallel with calorimetry measurements have been employed to characterize the as-quenched volume

of MSR samples. The kinetics behavior highlights the important role of the as-synthesized amorphous structure, modification of local structural arrangements, reaction pathways and transient conditions on the evolution of nanoscale microstructures during primary crystallization.

## *Scientific Progress and Accomplishments*

### Introduction

The current program has focused on understanding the dominant kinetic mechanisms that drive the primary nanocrystallization reaction in amorphous aluminum alloy as its primary objective. Amorphous aluminum alloys containing surprisingly high Al nc (nanocrystal) densities ( $10^{21} \text{ m}^{-3}$ ) have been found to exhibit unprecedented high strengths, making them potential materials for structural applications and providing the impetus to investigate the factors that control the nucleation and growth of ncs within the amorphous matrix. The main characteristics found from a number of examinations of primary crystallization in Al-based metallic alloys include an early development of a high Al nc nucleation density that increases modestly during continued reaction, and an Al nc size that exhibits sluggish growth.

At the highest reaction temperatures, growth may be inhibited by diffusion field impingement between neighboring Al nc, and throughout the reaction the partitioning of the low diffusivity rare earth component acts to limit growth. Experimental studies based only upon the standard Kolmogorov-Johnson-Mehl-Avrami type of analysis of calorimetric measurements cannot be applied directly to primary crystallization reactions as this standard approach neglects key information on the evolution of the nc size distribution during a reaction that is essential in the kinetics analysis. At the same time, a complete examination that correlates the calorimetric and related quantitative microstructural data that can be used to analyze the crystallization kinetics requires a clear description of the initial (i.e. as-quenched) state of the amorphous samples.

In the current period of research, effort has been focused on understanding the influence of varying annealing, alloying, and deformation treatments on the evolution of primary Al nanocrystals. Due to the inherent size scale associated with nanocrystals, investigations of the origin of nanocrystalline dispersions often require the use of transmission electron microscopy (TEM), atom probe field ion microscopy (APFIM), small angle X-ray scattering experiments (SAXS), and recently fluctuation electron microscopy (FEM) measurements [1, 2, 3]. In addition to microstructural characterization techniques, isothermal and continuous heating DSC experiments are proven techniques for conducting a kinetics analysis to distinguish between growth or nucleation and growth of primary phase crystallites. Although the amount of heat evolved from as-solidified marginal glass forming alloys due to growth of Al nanocrystals during isothermal DSC is often too small for detection by standard methods, microcalorimetry measurements coupled with TEM investigations completed during the current program demonstrate that Al nanocrystals experience growth during varying annealing treatments at temperatures below that associated with the onset of primary crystallization. In the case of the marginal glass forming alloy compositions investigated in this program (i.e.  $\text{Al}_{92}\text{Sm}_8$ ,  $\text{Al}_{87}\text{Ni}_{10}\text{Ce}_3$ , and  $\text{Al}_{88}\text{Y}_7\text{Fe}_5$ ), a clear glass transition signal is not evident during continuous heating of the as-solidified melt-spun ribbon samples. However, amorphous Al alloys synthesized by deformation methods have shown a clear glass transition signal along with the absence of a primary Al nanocrystallization reaction during a similar calorimetry analysis. Calorimetry results from other amorphous Al compositions (Al-Ni-Ce, Al-Fe-Gd, Al-Y-Fe, and Al-(Gd-X)-Ni) show behavior that is different from that for marginal glass forming compositions, exhibiting an exothermic peak only after an

observed incubation time during pre-crystallization isothermal annealing [reference]. These examples highlight the important role that processing conditions, thermal history, and small changes in composition can have on the interpretation of the observed kinetics behavior.

Although several methods have been developed to synthesize nanocrystal structures, crystallization from an amorphous matrix is the method that offers a most effective reaction control. This method has been used to develop nanocrystalline materials in several interesting categories that include the soft magnetic alloys [4], hard magnetic alloys [5], and high strength aluminum alloys [6]. Carefully designed microstructure fabrication techniques directly impact intrinsic property characteristics and hence material performance. Specifically, when compared to the tensile strength of amorphous aluminum alloys (~1000MPa), nanocrystalline Al-based alloys fabricated from an amorphous precursor have reportedly demonstrated tensile strengths up to 1500 MPa [7]. Since favorable mechanical properties usually arise from microstructures containing a high number density of small (5-10 nm) primary crystallites, an understanding of growth kinetics control will provide insight that will help identify microstructure synthesis routes to achieve the most favorable properties in these Al-based amorphous alloys.

In conjunction with calorimetry experiments, several nanocrystal size distribution analysis studies following TEM investigation of samples have characterized the primary crystallization kinetics of some amorphous Al alloys, showing the development of an early nanocrystal density that increases modestly as the reaction continues as well as a distinctly sluggish growth [1]. In other TEM investigations, size distributions of  $\alpha$ -Al

particles in Al-Y-Fe, Al-Ni-Nd, and Al-Ni-Y alloy systems were found to be consistent with those that would result from a transient heterogeneous nucleation mechanism [8, 9]. As a result, a large density (on the order of  $10^{21}$ - $10^{23}$  m<sup>-3</sup>) of heterogeneous sites is proposed to exist in the amorphous precursors, though their exact nature has yet to be determined.

In contrast to bulk glass forming alloys, amorphous Al alloys require rapid quenching for successful synthesis by solidification methods. The resulting marginal glass formation behavior represents a kinetic control based upon growth suppression. The same kinetic control also underlies the quench sensitivity that is evident from the reported crystallization studies. The common observation on the kinetics behavior suggests that heterogeneous nucleation is the governing mechanism, but other important characteristics such as the nature of the nucleation sites and the description of the kinetic rates are not currently resolved. While the technological significance of nanocrystalline microstructure design strategies is apparent, selected experimental tests and model kinetics analyses have been performed as one focus of the current program in order to address the fundamentals regarding the origin of the primary nanocrystallization reaction in the amorphous precursor material.

### Experimental Investigations

Primary crystallization reactions represent the key to achieving the microstructural designs associated with the most attractive structural properties, however these same reactions also appear to contribute to the marginal glass-forming behavior of Al-base systems. Indeed, based upon the comprehensive analysis developed by Inoue it is

clear that glass formation is favored for hypereutectic compositions [10]. For the hypereutectic composition range, it is somewhat unexpected that the kinetic competition during crystallization would favor the Al solution phase as the primary reaction product. For the most part the kinetic competition is largely determined by the relative magnitudes for the activation barrier for nucleation,  $\Delta G^*$ , which is proportional to  $(\sigma_{ls})^3/(\Delta G_v)^2$  where  $\sigma_{ls}$  is the liquid-solid interfacial energy and  $\Delta G_v$  is the driving free energy for nucleation. For primary crystallization that involves solute partitioning, the maximum value for  $\Delta G_v$  is determined by the parallel tangent construction [(11) reference]. Based upon the reported phase equilibria assessment for the Al-Sm system, the amorphous phase can be modeled as an undercooled liquid and both the Al solution and the  $Al_{11}Sm_3$  intermetallic phase have such a limited homogeneity range that they can be treated as line phases. The result of the parallel tangent analysis demonstrates that over the entire hypereutectic composition range of glass formation between 8 to 12 at% Sm, the  $Al_{11}Sm_3$  intermetallic phase is favored, yet the primary Al phase is observed.

In order to develop the analysis of relative driving free energy it is necessary to extrapolate the stable phase equilibria assessment to a highly undercooled condition. The extrapolation should include a heat capacity correction for the temperature dependence of the free energy. For an undercooled glass-forming alloy liquid, the heat capacity  $C_p^l$  has a non-linear temperature dependence and has not been measured over the entire undercooling range for Al-base amorphous alloys. There is a report of a  $\Delta C_p$  (i.e.  $C_p^l$  (liquid) -  $C_p$ (solid)) of about 12J/mole\*K for an Al-Ni-Ce alloy near  $T_g$ . This  $\Delta C_p$  is less than one-half of the value reported in the Au-Pb-Sb system where  $C_p^l$  measurements over a large fraction of the undercooling range indicate that  $\Delta G_v$  is reduced by about 10% due

to the  $\Delta C_p$  correction. On this basis, varying the thermodynamic solution model parameters to determine the influence of the  $\Delta G_V$  results reduced the extrapolated free energy values of the Al-Sm system. A 5% reduction in the liquid free energy changed the crossing point for the glass to Al and the glass to  $\text{Al}_{11}\text{Sm}_3$  from 5.3at% to 6.5at% Sm. This indicates that even after modifying the  $\Delta G_V$  values with a  $\Delta C_p$  correction that is consistent with reported measurements, the observed selection of primary Al suggests that there is a heterogeneous nucleation to favor the Al phase.

It is clear from the experimental results from the current program that the amorphous structure of the as-quenched alloy plays a vital role in determining its metastability (and subsequent crystallization character) [1, 12, 13]. An important result of the current research has been identification of the transient nature of the phase transformation in terms of both nucleation and growth. Marginal glass forming alloys have been reported to show a sensitivity to processing and indeed in many cases they illustrate a primary phase that is at a decided disadvantage as the first phase to nucleate in the crystallization scheme. With the usual diagnostic examination for glass formation based upon TEM observation and XRD, marginal glasses appear to represent true amorphous materials. However, it has become increasingly clear that closer examination reveals regions that may possess some ordered arrangements within the amorphous matrix. Small angle scattering and fluctuation microscopy suggest the presence of medium range order. These measurements do not clearly reveal all of the structural features or the chemical environment. Furthermore, some of the measurements are of a local type and do not account for a volume averaged behavior. At the same time, in many glasses, structural relaxation can take place at temperatures in the vicinity of the

glass transition. The relaxation events involve a local densification, and in some cases a change in chemical short range ordering as well. This has not been explored fully in the case of the marginal glass forming alloys although some relaxation response would be expected. Moreover, it is evident that any clustering or local structural change may represent a small volume of the sample and will require a high sensitivity and resolution for detection. In this regard nuclear magnetic resonance (NMR) offers an attractive option with a high sensitivity to local chemical environment and a capability of identifying different environments for a given component [14]

Primary crystallization is an important initial reaction during the devitrification of many metallic glasses. For example, in amorphous Al alloys the primary crystallization of a high number density of Al nanocrystals is associated with the attainment of exceptionally high tensile strength values. Experience indicates that the most favorable alloy compositions for Al-base glasses contain 85-92 at.% Al and remaining solute of either rare earth or transition metal components. In spite of the high Al content, all of the favored compositions are hypereutectic so that primary phase formation of Al is not favored. Instead, for hypereutectic compositions there is a decided driving free energy advantage to form an intermetallic phase as the primary crystallization product. The observed phase selection points to a heterogeneous nucleation reaction that promotes primary Al nucleation in spite of a driving free energy disadvantage. At the observed number densities of Al nanocrystals the particle separations are of the order of 100nm so that direct examination and identification of potential nucleation sites within the as-quenched amorphous alloy is difficult. There have been several reports where high resolution TEM has indicated the presence of irregular regions that appear to be Al

crystallites within an amorphous matrix [15, 16], although the identity of a possible precursor heterogeneity has yet to be identified with such electron microscopy techniques. Moreover, kinetics studies have established that the synthesis of the Al nanocrystal dispersion with number densities that exceed  $10^{22} \text{ m}^{-3}$  is governed by a heterogeneous nucleation process and can increase into the  $10^{23} \text{ m}^{-3}$  range with minor additions of Cu. At the highest number densities it is difficult to support a conventional heterogeneous nucleation model based upon catalysis by a foreign inclusion and indeed it appears that perhaps some local structural heterogeneity may be the source. Investigations of the initial structure of as-prepared amorphous Al-based alloys, and the thermally and/or mechanically induced microstructural evolution of these alloys, can yield results helpful in identifying the controlling mechanism for formation of microstructures consisting of high densities of Al nanocrystals in marginal Al glass forming alloys.

### SAXS

Small-angle x-ray scattering (SAXS) represents a fundamental method for structure analysis of condensed matter. The scattering of x-rays at small angles (close to the primary beam) provides structural information on inhomogeneities of the electron density with characteristic dimensions between one and a few hundred nm. For the current research program, SAXS experiments provide the opportunity to sample the size distributions of particles whose sizes remain below the resolution of conventional electron microscopy techniques ( $< 5 \text{ nm diam}$ ). SAXS measurements are conducted at the Argonne National Laboratory Advanced Photon Source in collaboration with Professor

Paul Evans at the University of Wisconsin-Madison.

An initial SAXS investigation of partially devitrified amorphous Al-Sm ribbons annealed at 130°C for 3 and 6 hours has been performed. **Figure 1a** shows the particle size distributions obtained for Al-Sm amorphous melt spun ribbons annealed for 3 and 6 hours respectively. As shown in these results, the first three hours of annealing accounts for three times the nucleation events that occurs in the second three hours. This is a clear indication that the nucleation rate is decreasing and is unfit for analysis using conventional steady-state nucleation theory. The negligible difference in average crystal size with increased annealing time indicates a growth kinetic limitation imposed by impinging diffusion fields between adjacent nanocrystals may be responsible for retarded growth at longer annealing times. The subsequent shifting of the crystal size distributions to larger values reflects dendritic growth, which represents a second growth mechanism. From a statistical standpoint, using small angle scattering to measure size distributions will allow particles beyond the capabilities of conventional TEM treatments to be resolved, resulting in a higher measured particle density- as shown in **fig. 1b**.

Compared to particle counting analysis of TEM micrographs, a more robust statistical analysis of data acquired from SAXS is possible due to the fact that SAXS is a volume averaging technique whereas TEM only probes a small 2-D slice of the microstructure. The SAXS technique provides confirmatory measurements that allow us to efficiently probe the evolving structure of marginal glasses at a large number of times and temperatures.

Fluctuational Microscopy

Nucleation sites for primary crystallization in melt-spun  $\text{Al}_{92}\text{Sm}_8$  metallic glass may be a form of nanometer length scale structural order, or medium-range order (MRO). Understanding the nature of this structure and how processing can modify it is important to tailoring the devitrification of high Al-content metallic glass. The potential for deviations from a dense random packed structure in real metallic glass samples is also of significant fundamental interest.

Fluctuation electron microscopy (FEM) is a technique to quantitatively detect MRO in amorphous materials [17, 18]. FEM uses hollow-cone dark field imaging in a transmission electron microscope (TEM) to measure diffraction from nanoscale volumes of the sample. As the electron beam is tilted, pockets of structural order will meet a Bragg condition and strongly scatter electrons; an excited Bragg condition will generate a bright spot in a dark field micrograph compared to the amorphous matrix. If there are more ordered regions in the sample (more MRO), there will be more bright spots in the image. If the beam is tilted between Bragg conditions, the ordered pockets will appear particularly dark. Overall, the more speckle of bright and dark areas that appear in a dark field micrograph, the more MRO is present in the sample. The specific size of MRO clusters measured by the FEM method is dependent upon the size of the objective aperture in place in the TEM [18]. At present, the spatial resolution limit (governed by the electron microscopy equipment available at UW-Madison) of the FEM technique is 16Å.

FEM investigations on amorphous  $\text{Al}_{92}\text{Sm}_8$  prepared by melt-spinning and cold-rolling of elemental foils have shown distinct differences in type and degree of medium range order (MRO) in the amorphous phase (**Fig. 2**) suggesting that the MRO may be a

precursor to primary crystallization, thus differentiating the crystallization mechanism in amorphous samples prepared by different processing routes [3].

### Chemically Catalyzed Primary Crystallization

Selective substitutions of Cu for Ni in  $\text{Al}_{88}\text{Ni}_{8-x}\text{Sm}_4\text{Cu}_x$  melt-spun ribbon samples ( $x = \text{at\% Cu}$ , ranging from 0.2  $\rightarrow$  1at%) shift the calorimetrically measured onset of primary crystallization to successively lower temperatures with increasing amount of Cu substitution (**figure 3**). The integrated enthalpy of the primary crystallization exotherm (normalized by sample mass) does not change appreciably with Cu substitution level indicating that the volume of amorphous precursor material transforming to primary Al nanocrystals remains essentially constant with changes in Cu substitution level. Further, the shape of the primary exothermic onset changes from a sharp deviation from a horizontal baseline to a more shallow depression extending over a wider temperature range.

Microstructure analysis of ribbon samples of  $\text{Al}_{88}\text{Ni}_8\text{Sm}_4$  and  $\text{Al}_{88}\text{Ni}_7\text{Sm}_4\text{Cu}_1$  annealed for 30 minutes at the onset of primary crystallization for each composition (estimated with DSC to be 154 and 104°C respectively) indicate that the average size of the primary phase nanocrystals is reduced by nearly 25% with Cu substitution (**figure 4**). Instead of applying a traditional histogram method to analyze the nanocrystal size distribution, the measured nanocrystals were ranked according to size, and the subsequent cumulative distribution function was plotted as a function of nanocrystal size [1]. Further, by applying an accurate lognormal fit to the probability density function (coarse derivative of the c.d.f.) mean and standard deviation values for each composition are

established. By virtue of applying electron energy loss spectroscopy (EELS) to estimate the sample thickness, the nanocrystal density per volume was calculated with

$$N_v = \frac{N_A}{t + d}$$

where  $N_A$  is the nanocrystal density per micrograph assuming that the nanocrystal diameter  $d$  is small relative to the sample thickness  $t$  [19]. The estimated nanocrystal density increased from  $9 \cdot 10^{21}$  to  $1.6 \cdot 10^{22} \text{ m}^{-3}$  with substitution of 1at% Cu for Ni in the base alloy composition. These estimates were based on analysis of a composite micrograph obtained by overlaying four separate DFTEM micrographs taken with the objective aperture placed at four symmetric clock positions around the primary diffraction ring.

Unlike the previously reported behavior of catalytic effects of small Cu additions in Fe-based glasses, atom probe results have shown that in Al-based glasses containing small amounts of Cu, the Cu atoms are distributed homogeneously in the amorphous matrix [20]. Since TEM and atom probe analyses have not yet provided a conclusive explanation of how the small Cu substitutions refine the grain size in amorphous Al-based alloys, further calorimetry investigations were performed to explore whether the broad shape of the primary crystallization exotherm present in the  $\text{Al}_{88}\text{Ni}_7\text{Sm}_4\text{Cu}_1$  could be due to crystallization events driven by multiple heterogeneities (i.e. Al clusters retained during the quench and/or Cu atoms or clusters).

The gradual broadening of the primary crystallization onset with increased Cu substitution level suggests that independent primary crystallization events may be taking

place over a broad temperature range, with the earliest nucleation events being catalyzed by a more potent heterogeneity than is present in the alloy containing no Cu. To explore this hypothesis, replicate as-solidified  $\text{Al}_{88}\text{Ni}_7\text{Sm}_4\text{Cu}_1$  ribbon samples were heated to  $120^\circ\text{C}$  and annealed for 0, 10, and 30 minutes respectively. Following the annealing treatment, the samples were immediately quenched to room temperature, and then reheated through crystallization. By comparing the change in primary crystallization enthalpy between the as-solidified sample and each annealed sample, the fraction of material transformed from the amorphous precursor phase to primary Al nanocrystals was estimated. Balancing the enthalpy of primary crystallization of the as-spun alloy with the total enthalpy of crystallization (primary and intermetallic), it is determined that approximately 40% of the total exothermic enthalpy results transformation to  $\alpha$ -Al (a *rough* measure of the material volume transformed). The data in **figure 5** indicates that there is an initial burst of nucleation during a cycle around  $120^\circ\text{C}$  (isothermal holding time = 0 min.) whereby 7.1% of the material has transformed to Al nanocrystals. Following 10 and 30-minute isothermal holding treatments at  $120^\circ\text{C}$ , an additional 1.8 and 6.8% (respectively) of the microstructure transforms to primary Al nanocrystals. These results indicate that upon heating the as-solidified material from room temperature to the isothermal annealing temperature ( $120^\circ\text{C}$ ) at  $20^\circ\text{C}/\text{min}$ , nearly the same volume of material transforms from the amorphous precursor phase to primary Al nanocrystals as transforms during the 30 minute annealing treatment at  $120^\circ\text{C}$ . Complementing the TEM size distribution results, it is evident that nucleation of a high density of primary phase nanocrystals is catalyzed at low temperatures (when diffusion is slow) by a heterogeneity not present in the base composition without Cu. The broadening of the primary

crystallization exotherm and the reduction of mean nanocrystal size (with a narrowed size distribution) with the substitution of 1at% Cu for Ni in this alloy system are original characteristics that imply that the presence of Cu restricts growth of the primary phase. In a similar Al-based alloy system, APFIM work indicates that there is extensive build up of the slowly diffusing rare earth element at the interface between the nanocrystal and amorphous matrix [2], however no further structural studies conclusively indicate that Cu atoms are preferentially redistributed at the nanocrystal interface during primary phase crystallization. Growth restriction of the primary phase as a result of RE atom pile-up at the interface can explain why there is little growth of  $\alpha$ -Al nanocrystals following the initial burst of nucleation during heating to the annealing temperature, however further studies must be completed to clarify how the presence of small amounts of Cu can restrict n.c. growth even further.

Another interesting feature of the DSC traces of  $\text{Al}_{88}\text{Ni}_7\text{Sm}_4\text{Cu}_1$  following incremental annealing treatments at  $120^\circ\text{C}$  is the markedly sharp exothermic departure of the calorimetry trace from the horizontal baseline. Although the heating trace of the as-solidified alloy deviates from the baseline at  $\sim 104^\circ\text{C}$ , this result emphasizes that there are multiple nucleation events occurring over the broad primary crystallization exotherm thus suggesting the presence of heterogeneities of varying potency in the as-quenched solid. Preliminary fluctuation electron microscopy (FEM) measurements on as-quenched  $\text{Al}_{88}\text{Ni}_8\text{Sm}_4$  and  $\text{Al}_{88}\text{Ni}_7\text{Sm}_4\text{Cu}_1$  MSR samples indicates a distinct difference in the medium range order, further suggesting that small levels of Cu substitution can affect the structure of the amorphous solid, thus causing a change in primary crystallization behavior [21].

## *Summary*

From the progress and results that have been achieved during the current program, several new aspects of solidification and amorphization under high undercooling conditions and deformation-induced transitions have emerged that warrant further study and analysis. One area of central interest is the further examination of the early stage evolution of nanocrystals, to develop a clear understanding of the controlling nucleation and growth kinetics. The initial findings in the current research indicate that a non steady state growth rate, that may reflect concurrent relaxation, contributes to the reaction, which will require further experiments to quantify and model. It seems highly probable that the source of the transformation kinetics behavior stems from the as quenched state. In order to build on these accomplishments and new capabilities, another focus of the intended program will be to apply structural and calorimetric analyses to understand the as-quenched state of the amorphous sample, and to quantify the effect of quenched in features on the primary phase nanocrystallization kinetics. The overarching goal is to identify a means to process – through thermal, chemical, or mechanical treatments – as-quenched marginal glasses so as to achieve a reproducible initial state for the material and to allow for prediction of the evolution of primary phase nanocrystals based upon a given driving force. With this new capability it will be possible to synthesize nanoscale microstructures in bulk volumes that provide exceptional levels of performance for structural applications.

## References

1. J. H. Perepezko, R. J. Hebert, W. S. Tong, J. Hamann, H. R. Rösner and G. Wilde: Mater. Trans. JIM **44**, 1982-1993 (2003).
2. K. Hono et al., Scripta Met., 32, 2 (1995).
3. W. G. Stratton, J. Hamann, J. H. Perepezko, P. M. Voyles, X. Mao, S. V. Khare, Appl. Phys. Lett. **86** (14) 141910 (2005).
4. C. C. Koch: Nanostruc. Mater. **2** (1993) 109.
5. A. Manaf, R. A. Buckley and H. A. Davies: J. Magn. Magn. Mater. **128** (1993) 302.
6. Y. H. Kim, K. Hiroga, A. Inoue, T. Masumoto and H. H. Jo: Mater. Trans. JIM, **35** (1994) 293.
7. A. Inoue, Y. Horio, Y. H. Kim and T. Masumoto: Mater. Trans. JIM **33** (1992) 669.
8. P. Rizzi, M. Baricco, L. Battezzati, P. Schumacher and A. L. Greer: Materials Science Forum **235-238** (1997) 409.
9. D. R. Allen, J. C. Foley and J. H. Perepezko: Acta Mater. **46** (1998) 431.
10. A. Inoue: Progr Mat Sci **43** (1998) 365.
11. M. Grujicic: Calphad **13** (1989) 205.
12. R. J. Hebert and J. H. Perepezko, Scripta Materialia, **50**, 807-812 (2004).
13. J. H. Perepezko, Progress in Materials Science, **49**, 263-284 (2004).
14. J. H. Perepezko, J. Hamann, Y. Wu, *private discussion*.

15. T. Gloriant, D. H. Ping, K. Hono, A. L. Greer, M. D. Baró, *Mat. Sci. & Eng.* A304-306, 315, (2001).
16. G. Wilde, H. Rösner, J. Hamann, W. S. Tong, J. H. Perepezko, *Mat. Res. Soc. Symp. Proc.*, 806, 33, (2004).
17. M. M. J. Treacy and J. M. Gibson, *Acta Cryst. A* 52, 212 (1996).
18. P. M. Voyles, J. M. Gibson, and M. M. J. Treacy, *J. Electron Microsc.* 49, 259 (2000).
19. J. Hamann, W.S. Tong, J.H. Perepezko, to be published.
20. Y. Zhang, P.J. Warren, A. Cerezo, *Mat. Sci. & Engr.* **A327**, 109 (2002).
21. W.G. Stratton, J. Hamann, J.H. Perepezko, P.M. Voyles, *private discussion*.

Figures

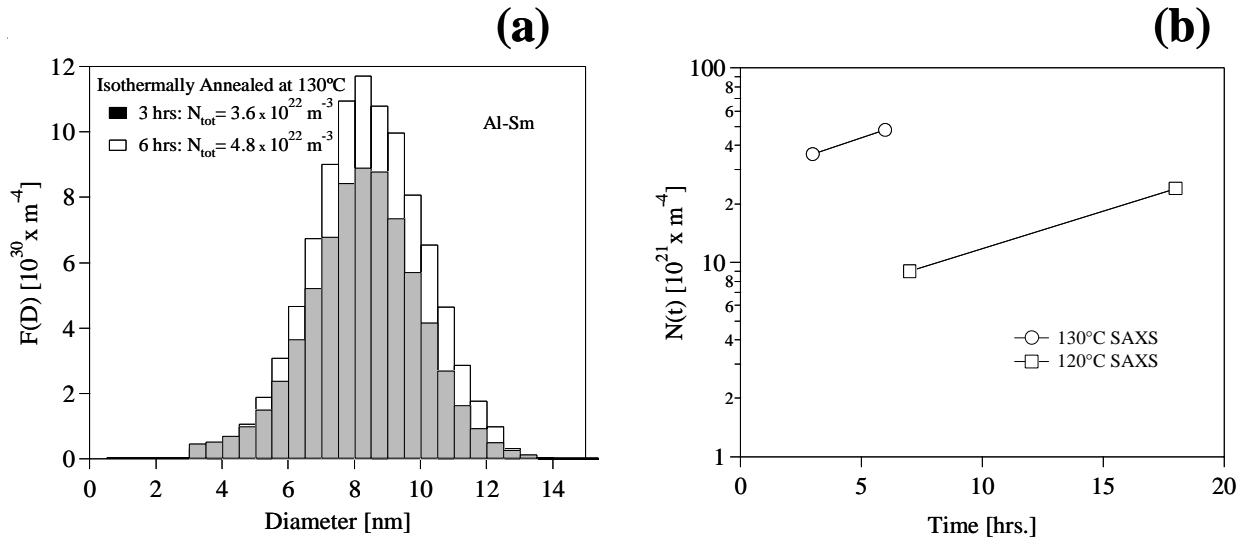


Figure 1. (a) Particle size distributions obtained for Al-Sm amorphous melt spun ribbons annealed for 3 and 6 hours respectively. (b) measured number densities,  $N$ , measured from SAXS at 120° and 130° for different annealing times and different analysis methods.

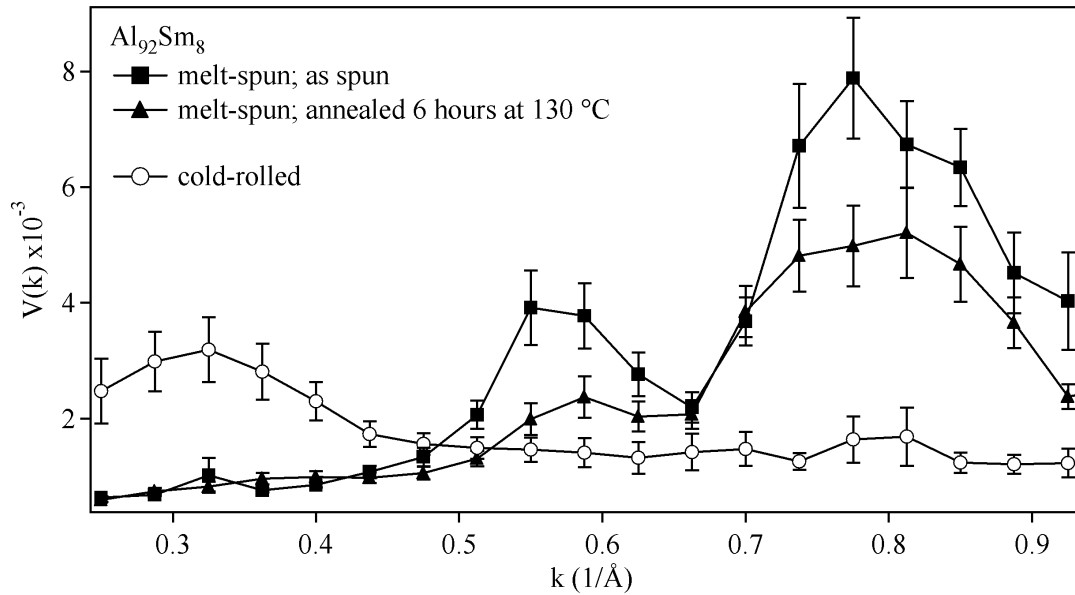
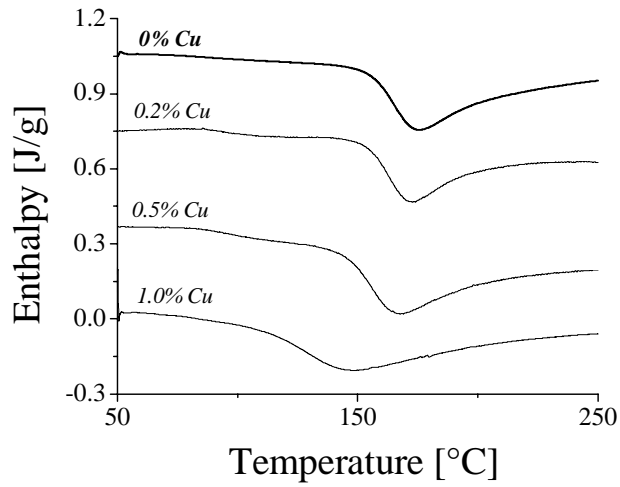


Figure 2:  $V(k)$  for melt-spun as-spun, melt-spun annealed, and cold-rolled  $\text{Al}_{92}\text{Sm}_8$  metallic glass. The peak locations in the as-spun and annealed samples are the same, showing that the same type of MRO is present in both samples. The height of the peaks decreases, indicating a decrease in the degree of MRO. The cold-rolled samples shows a lower peak in a different location, indicating it has less MRO of a different type than the either melt-spun sample.



$X_{Cu}$ [at%]	$\Delta H_x$ [J/g]
0	77.5
0.2	78.2
0.5	76.4
1	77.3

Figure 3: DSC traces ( $dT/dt = 20^\circ\text{C}/\text{min}$ ) of  $\text{Al}_{88}\text{Ni}_{8-x}\text{Sm}_4\text{Cu}_x$  MSR samples; as the crystallization onset shifts to lower temperatures with greater Cu substitution, the integrated crystallization enthalpy remains constant.

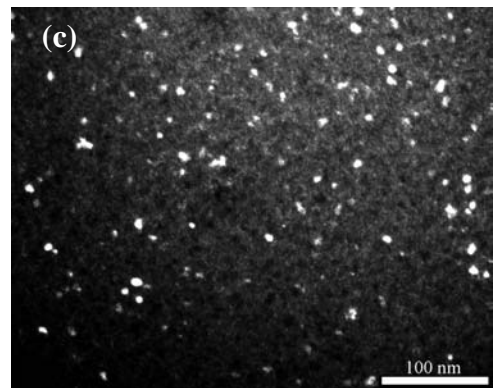
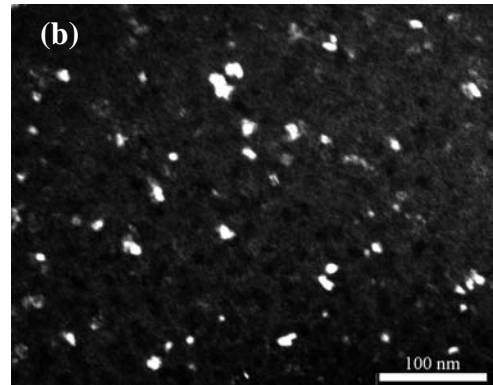
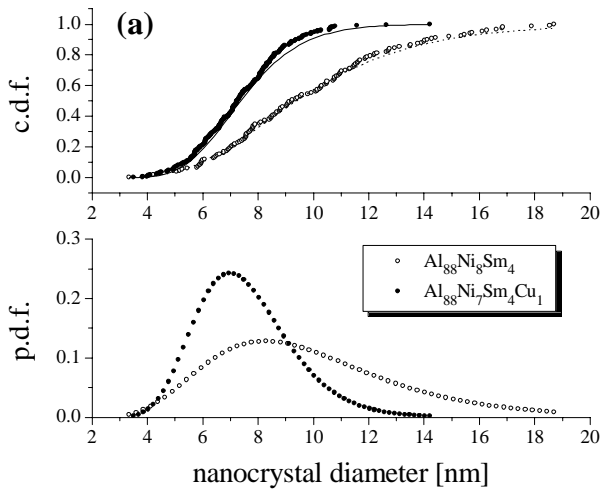
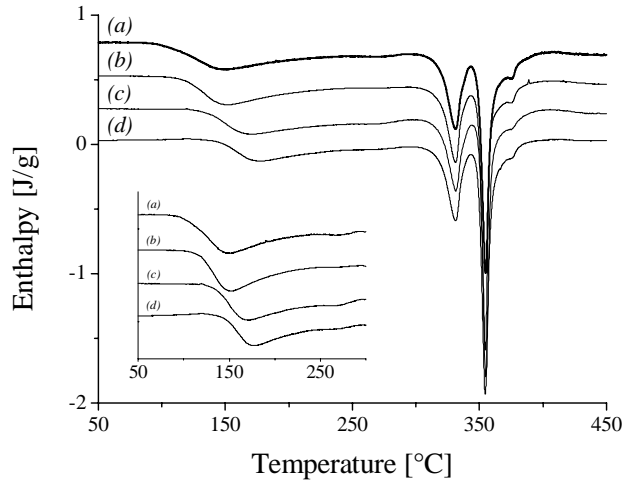


Figure 4: (a) cumulative and probability density functions showing the distribution of  $\alpha$ -Al n.c.'s; DFTEM micrographs of  $\alpha$ -Al nc's in (b)  $\text{Al}_{88}\text{Ni}_8\text{Sm}_4$  and (c)  $\text{Al}_{88}\text{Ni}_7\text{Sm}_4\text{Cu}_1$



(a) as-spun  
 (b) cycled around 120°C  
 (c) 10min anneal at 120°C  
 (d) 30min anneal at 120°C

Annealing time at			
120°C [min]	T <sub>x</sub> [°C]	ΔH <sub>x</sub> [J/g]	f <sub>x</sub> tal
as-spun	103	77.5	--
0	115	64.9	7.1%
10	133	61.7	8.9%
30	144	52.9	13.9%

Figure 5: Continuous heating DSC traces of Al<sub>88</sub>Ni<sub>7</sub>Sm<sub>4</sub>Cu<sub>1</sub> following thermal cycling treatments around 120°C. Also included is a summary of the integrated crystallization enthalpies and subtracted DSC traces to illustrate how the annealing treatments affect the primary crystallization behavior.

## ***PUBLICATIONS OF THE CURRENT PROGRAM***

During a research program, substantial time intervals often elapse between the completion of a research study, submission of a manuscript and the final appearance of a paper in print. As a result, the following list gives publications in preparation as well as those in print or in press. (The papers noted by an asterisk are invited). Interim reports for this grant were submitted to the ARO in 2002, 2003, and 2004.

22. "Solid State Amorphization by Cold Rolling", H. Sieber, G. Wilde, A. Sagel and J. H. Perepezko, EUROMAT 2000, Materials Development and Processing-Bulk Amorphous Materials, Undercooling and Powder Metallurgy, **8**, 3, (2000).
23. "Intermetallic Phase Formation in Bulk Multilayered Structures", H. Sieber and J. H. Perepezko, EUROMAT 2000, Intermetallics and Superalloys, **10**, 324, (2000).
24. "Nucleation Kinetics Analysis by Repeated Solidification of Single Droplets", G. Wilde, J. Sebright, P. Hockel and J. H. Perepezko, EUROMAT 2000, Materials Development and Processing-Bulk Amorphous Materials, Undercooling and Powder Metallurgy, **8**, 85, (2000).
25. "Superheating" J.H. Perpezko, The Encyclopedia of Mat. Sci. and Technology, Eds. K.H.J. Buschow, R.W. Cahn, M.C. Flemmings, B. Ilschner, E.J. Kramer, and S. Mahajan, Elsevier (Oxford), 8975, (2001).
26. "Low temperature, mercury-mediated synthesis of aluminum intermetallics", M. Khoudiakov, A. B. Ellis, J. H. Perepezko, S. Kim and K. D. Kepler, Chemistry of Materials, **12**, 2008-2013 (2000).
27. "Amorphization and alloy metastability in under-cooled systems", J. H. Perepezko and G. Wilde, J. Non-Cryst. Solids, **274**, 271-281 (2000).
28. "Kinetics of glass formation and nanocrystallization in Al-RE-(TM) alloys", R. I. Wu, G. Wilde and J. H. Perepezko, Minerals, Metals and Materials Society/AIME, Ultrafine Grained Materials, p63-72, (2000).
29. "Cold-rolling of Al-based alloys", R. J. Hebert, G. Wilde, H. Seiber and J. H. Perepezko, Minerals, Metals and Materials Society/AIME, Ultrafine Grained Materials, 165-172, (2000).
30. "Liquidus and temperature determination in multicomponent alloys by thermal analysis", R. I. Wu and J. H. Perepezko, Met. Mat. Trans., **31A**, 497-501 (2000).
31. "Glass formation and nanostructure development in Al-based alloys", R. I. Wu, G. Wilde, and J. H. Perpezko, Mat. Res. Soc. Symp., Vol, 101-106 (2000).
32. "Nanostructure formation by rapid solidification and solid state processing", R. I. Wu, R. J. Hebert and J. H. Perepezko, ASM International, Understanding Processing, Structure, Property, and Behavior Correlations, **27**, 12, (2000).
33. "Glass formation and primary nanocrystallization in Al-base metallic glasses", J. H. Perepezko, R. I. Wu, and G. Wilde, Mat. Sci. & Engr. A., **301**, 12-17 (2001).
34. "Undercooling and glass formation in Al-based alloys", S. K. Das, J. H. Perepezko, R. I. Wu and G. Wilde, Mat. Sci. & Engr. A, **304-306**, 159-165, (2001).
35. "Synthesis and stability of amorphous Al alloys", J. H. Perepezko, R. I. Wu, R. Hebert and G. Wilde, Mat. Res. Soc. Symp. (2001)

36. "Amorphous aluminum alloys- synthesis and stability" J. H. Perepezko and R. J. Hebert, *JOM*, **54**, 34-39 (2002).
37. "The significance of the heat of mixing for the amorphization of multilayers by deformation processing" R. J. Hebert and J. H. Perepezko, *Materials Science Forum*, **386-388**, 21-26 (2002).
38. "Nanostructure synthesis and amorphization during cold rolling", J. H. Perepezko, R. J. Hebert and R. I. Wu, *Materials Science Forum*, **386-388**, 11-20 (2002).
39. "Heterogeneous microstructural evolution and reaction during repeated intense deformation", R. J. Hebert and J. H. Perepezko, *Ultrafine Grained Materials II*, Eds. Y.T. Zhu, T.G. Langdon, R.S. Mishra, S.L. Semiatin, M.J. Saran, and T.C. Lowe (TMS, Warrendale, PA), 141, (2002).
40. "Initial crystallization kinetics in undercooled droplets", J. H. Perepezko, P. G. Hockel and J. S. Paik, *Thermochimica Acta*, **388**, 129-141 (2002).
41. "Amorphization and nanostructure synthesis in Al alloys" J. H. Perepezko, R. J. Hebert and W. S. Tong, *Intermetallics*, **10**, 1079-1088 (2002).
42. "Undercooling and solidification of atomized liquid droplets", J. H. Perepezko, J. L. Sebright, P. G. Höckel and G. Wilde, *Mat. Sci. & Engr. A*, **326**, 144-153, (2002).
43. "Solidification of atomized liquid droplets", J. H. Perepezko, J. L. Sebright and G. Wilde, *Adv. Engr. Mat.*, **4**, 147-151, (2002).
44. "Primary crystallization in amorphous Al-based alloys", J. H. Perepezko, R. J. Hebert, R. I. Wu, and G. Wilde, *Journal of Non-Crystalline Solids*, **317**, 52-61 (2003).
45. "Nucleation-catalysis-kinetics analysis under dynamic conditions", J. H. Perepezko and W. S. Tong, *Philosophical Transactions of the Royal Society of London Series A*, **361**, 447-460 (2003).
46. "Nanocrystallization in Al-rich metallic glasses", G. Wilde, N. Boucharat, R. J. Hebert, H. Rösner, W. S. Tong and J. H. Perepezko, *Advanced Engineering Materials*, **5**, 125-130 (2003).
47. "Nanometer-scale solute clustering in aluminum-nickel-ytterbium metallic glasses", D. Isheim, D. N. Seidman, J. H. Perepezko, G. B. Olson, *Materials Science and Engineering A*, **353**, 99-104 (2003).
48. "Structural transformations in crystalline and amorphous multilayer samples during cold-rolling", R. J. Hebert and J. H. Perepezko, *Scripta Mat.*, **49**, 933-939 (2003).
49. "Nanocrystallization Reactions in Amorphous Aluminum Alloys", J. H. Perepezko, R. J. Hebert, W. S. Tong, J. Hamann, H. R. Rösner and G. Wilde: *Mater. Trans. JIM* **44**, 1982-1993 (2003).
50. "Deformation-induced crystallization and amorphization of Al-based metallic glasses", R. J. Hebert and J. H. Perepezko, *Mat. Res. Soc. Symp.*, **754**, 267-272 (2003).
51. "Analysis of primary crystallization in amorphous aluminum alloys", J. H. Perepezko, W. S. Tong, J. Hamann, R. J. Hebert, H. R. Rösner and G. Wilde, *Mat. Res. Soc. Symp. Proc.*, **754**, 347-352 (2003).

52. "Deformation-induced synthesis and structural transformations of metallic multilayers", R. J. Hebert and J. H. Perepezko, *Scripta Materialia*, **50**, 807-812 (2004).
53. "Nucleation-controlled reactions and metastable structures," J. H. Perepezko, *Progress in Materials Science*, **49**, 263-284 (2004).
54. "Medium-Range Order in High Al-content Amorphous Alloys Measured by Fluctuation Electron Microscopy", W.G. Stratton, J. Hamann, J.H. Perepezko, P.M. Voyles, *Mat. Res. Soc. Symp. Proc.*, **806**, 275-280 (2004).
55. "Early stages of Al-nanocrystal formation in Al<sub>92</sub>Sm<sub>8</sub>", G. Wilde, H. Rösner, J. Hamann, W.S. Tong, J.H. Perepezko, *Mat. Res. Soc. Symp. Proc.*, **806**, 33-38 (2004).
56. "Effect of Cold-rolling on the Crystallization behavior of Amorphous Al<sub>88</sub>Y<sub>7</sub>Fe<sub>5</sub> Alloy", R. J. Hebert, J. H. Perepezko, *Mat. Sci. & Engr* **A375-377**, 728-732 (2004).
57. "Devitrification of Al-based Glass Forming Alloys", N. Boucharat, H. Rösner, J. H. Perepezko, G. Wilde, *Mat. Sci. & Engr* **A375-377**, 713-717 (2004).
58. "Thermally Controlled Nanocrystallization in Amorphous Al Alloys", J. Hamann, W. S. Tong, H. Rösner, J. H. Perepezko and G. Wilde, *Solid State Phenomena*, **101-102**, 259-264 (2005).
59. "Aluminum nanoscale order in amorphous Al<sub>92</sub>Sm<sub>8</sub> measured by fluctuation electron microscopy", W. G. Stratton, J. Hamann, J. H. Perepezko, P. M. Voyles, X. Mao, S. V. Khare, *Appl. Phys. Lett.* **86** (14) 141910 (2005).
60. "Primary Nanocrystallization and Amorphous Alloy Stability", J. H. Perepezko, R. J. Hebert, *J. Non-Equilib. Processing*, *accepted*.
61. "Deformation-induced mixing reactions in Cu-Cd multilayers", R. J. Hebert, G. Wilde, J. H. Perepezko, *J. Non-Equilib. Processing*, *accepted*.
62. "Amorphization and devitrification reactions in metallic glass alloys", J.H. Perepezko, J. Hamann, R.J. Hebert, H. Rösner, G. Wilde, *Mat. Sci. & Engr. A*, *accepted*.
63. "The Effect of As-quenched Structure on Primary Phase Crystallization in Amorphous Aluminum Alloys", J. Hamann and J. H. Perepezko, *Mat. Res. Soc. Symp. Proc.*, *accepted*.

*Scientific Personnel*

Professor John H. Perepezko, Principal Investigator  
Rainer Hebert, Ph.D conferred 2003  
Joseph Hamann, M.S. conferred 2003  
Dr. William Scott Tong